Capacitive detection of magnetic field induced quantum phase transitions in an imbalanced bilayer electron system

S. I. Dorozhkin, A. A. Kapustin ⬤, and I. B. Fedorov
Institute of Solid State Physics RAS, 142432 Chernogolovka, Moscow District, Russia

V. Umansky ⬤
Department of Condensed Matter Physics, Weizmann Institute of Science, 76100 Rehovot, Israel

J. H. Smet ⬤
Max-Planck-Institute für Festkörperforschung, Heisenbergstrasse 1, D-70569 Stuttgart, Germany

Ground states that appear in a quantizing magnetic field in an imbalanced bilayer electron system hosted by a dual-gated, wide GaAs quantum well are explored with a magnetocapacitance technique that enables detection of the compressibility of each layer separately, the characterization of the charge distribution, as well as the distinction of single- or double-layer-like behavior. Magnetic field induced reentrant quantum phase transitions are observed between a compressible double-layer ground state and a single-layer-like incompressible phase for both total fillings 1 and 2. The transitions are accompanied by a charge redistribution across the well. Our observations indicate for both incompressible states easy-plane pseudospin ferromagnetism as the origin.

I. INTRODUCTION

Electron-electron interactions play a crucial role for some integer quantum Hall (QH) states in bilayer electron systems (BLESs). Many-body ground states were predicted and experimentally studied when the total electron density equals the degeneracy of a single spin-split Landau level or twice this value, i.e., at *total* filling factor $\nu = 1$ and 2. Most attention has been paid to the $\nu = 1$ state where an exciton condensate forms as demonstrated in a series of pioneering experimental works [1–6]. At $\nu = 2$, three phases with distinct spin polarization have been predicted, one of which, the canted antiferromagnetic phase, is entirely due to electron-electron interactions [7–10]. Extensive experimental studies based on inelastic light scattering [11,12], magnetotransport [13–15], magnetocapacitance [16], and nuclear magnetic resonance [17,18] were argued to be consistent with the canted antiferromagnetic phase.

Most previous theoretical and experimental studies deal with double-quantum-well (DQW) samples, where the two electron layers are separated by an *in situ* grown barrier. Such systems are easier to treat in theory than bilayer systems that form in a wide quantum well (WQW), with the layers located on opposite sides of the well and separated by a barrier that

forms self-consistently due to Coulomb repulsion [19]. In DQW samples it is possible to contact the individual layers [20], which greatly expands the accessible experimental information.

According to theory, exchange-correlation effects in DQW BLESs become prominent when two single-particle Landau levels, one of each layer, are brought into coincidence at the electrochemical potential and when these two levels are partially occupied such that the total number of electrons corresponds to complete occupation of only one of the levels. Then the single-particle picture with Landau ladders fails, and a many-body gap appears in the energy spectrum of the entire system, resulting in a QH state. This physics is commonly addressed by introducing the pseudospin as an additional degree of freedom describing the location of an electron in either one of the layers. The incompressible ground state is then attributed to pseudospin ferromagnetism [9,21,22]. Its many-body wave function consists of a superposition of the wave functions of the aligned levels, which can result in interlayer coherence even in the absence of tunneling between the layers [23]. In WQW samples at $\nu = 2$ and 4, an alternative possibility for the appearance of an incompressible ground state has been raised [24], triggered by the experimental observation of hysteresis. A first-order phase transition may occur where electrons of the aligned levels all reside in one layer and subsequently switch layer. In the pseudospin language, such a transition is a manifestation of easy-axis anisotropy, whereas interlayer coherent states reflect easy-plane anisotropy. The origin of easy-axis anisotropy in WQWs is the softness of the barrier [24]. The emergence of pseudospin ferromagnetic QH states is expected to be accompanied by a redistribution of charge in the quantum well. This redistribution has so far

not been explored. This represents one important goal of this work.

Here we have carried out magnetocapacitance experiments on a bilayer electron system that forms in an asymmetric GaAs WQW. We employ the method reported in Ref. [25], which allows (i) to measure the compressibility of the individual layers (which represent electrical subbands in the imbalanced BLES) despite the absence of separate contacts to each layer, (ii) to identify charge redistributions within the well, as well as (iii) to observe the level alignment of the different layers, even in the compressible regime where some of this information is impossible to obtain from magneto-transport. Such a technique has been deployed in double-layer graphene samples in Ref. [26]. We demonstrate that in order to establish equilibrium in the imbalanced BLES, the system favors a coincidence of the Landau levels belonging to different layers at the electrochemical potential level. The partial occupation of both levels then gives rise to double-layer-like ground states with compressible behavior. They are interrupted at $\nu = 1$ and 2 due to a quantum phase transition to an incompressible single-layer-like state with easy-plane pseudospin anisotropy. The apparently similar underlying physics observed at $\nu = 1$ and 2 was unexpected in view of the previous interpretation of transport data in WQW samples at $\nu = 2$, which were explained in terms of easy-axis pseudospin ferromagnetism instead [24]. Our results for the reentrant quantum phase transitions partly overlap with recent findings of the interplay between double- and single-layer-like behavior in a nominally balanced WQW bilayer unveiled in composite fermion geometric resonances in the vicinity of $\nu = 1$ and $1/2$ [27,28].

II. EXPERIMENTAL DETAILS

Our studies were performed on two identical samples processed in the Hall bar geometry side by side on the same wafer piece of a GaAs/AlGaAs heterostructure. The heterostructure hosts a 60-nm-wide GaAs quantum well which is located 140 nm below the crystal surface and comprises the studied electron system. The front electron layer (FL) arises at the top GaAs/AlGaAs interface and is populated with electrons through conventional modulation doping from Si donors located 65 nm above the quantum well in an AlGaAs barrier, similar to the two-dimensional electron systems (2DESs) at a single GaAs/AlGaAs heterointerface. Its electron density n_{FL} can be tuned with a voltage V_{FG} applied to a front gate consisting of a CrAu film deposited on the crystal surface and covering about 95% of the device area. At $V_{FG} = 0$, $n_{FL} = 1.8 \times 10^{11}$ cm^{-2} and the low-temperature mobility is equal to $\mu_{FL} = 11 \times 10^6$ cm^2/Vs. An *in situ* grown, heavily doped GaAs layer at a distance of 850 nm below the quantum well serves as a back gate and allows to create the back 2D layer (BL) at the bottom heterointerface by applying a back gate voltage $V_{BG} > 0.15$ V. When both layers are occupied, the variation of the front (back) gate voltage affects the electron density almost only in the front (back) layer. The capacitances between both gates and the electron system were measured simultaneously with the use of two dual-phase lock-in amplifiers by modulating the gate voltages at different ac frequencies and measuring the out-of-phase components

of an ac current of these two frequencies flowing to the electron system. To minimize the stray capacitance, the gates were connected to coaxial cables. Further experimental details can be found in Ref. [25]. The magnetoresistance and Hall resistance were measured with the use of the conventional ac technique. The sample was immersed in liquid ^{3}He. Its temperature was set by pumping the ^{3}He vapor and controlling its pressure ($0.5 \leqslant T < 1.5$ K) or the ^{4}He vapor pressure ($1.5 \leqslant T < 4.2$ K) of a 1-K pot.

III. EXPERIMENTAL RESULTS AND DISCUSSION

Figure 1 illustrates typical *B*-field dependencies at 0.5 K of the capacitance between the electron system and the front (C_{FG}) and back gate (C_{BG}), respectively, together with magnetotransport data for two different V_{BG} and a fixed V_{FG} of -0.2 V. For these two back gate voltages, the density in the front layer is nearly the same, while the back layer occupation is different. Rather than plotting the recorded $C_j(B)$ (here j refers either to FG or BG), corrected and normalized capacitances, referred to as $C_{j,norm}(B)$, are shown instead. They were obtained by first subtracting constant parasitic capacitances $C_{j,par}$ composed of two contributions: field-independent stray capacitances as well as a capacitance contribution originating from the device region not covered by the front gate. The latter is only relevant for C_{BG} and is in principle *B* dependent. Here we use the constant value obtained when the region underneath the front gate is incompressible. We defer more details to the Supplemental Material [29]. Subsequently, the corrected capacitance values were normalized to those at zero field:

$$C_{j,norm}(B) = [C_j(B) - C_{j,par}]/[C_j(B = 0) - C_{j,par}]. \quad (1)$$

For the studied sample, we obtain $C_{FG}(B = 0) = 279$ pF, $C_{FG,par} = 13$ pF, $C_{BG}(B = 0) = 70.2$ pF, and $C_{BG,par} = 26.3$ pF. The presented normalized capacitance $C_{j,norm}$ traces display various minima. Similar to conventional field effect transistors, these minima reflect a reduced compressibility of a two-dimensional electron system (2DES) [30], a quantity proportional to its thermodynamic density of states D. Here we will mainly consider minima at integer filling factors when the chemical potential lies in a gap separating two Landau levels of the total electron system or just the front or back layer. Four different types of minima can be distinguished. The deepest minima (type I), appearing simultaneously in $C_{FG,norm}$ (black) and $C_{BG,norm}$ (red), occur when the entire BLES condenses in an incompressible ground state at $\nu = 1$ or 2 with participation of all electrons as confirmed by quantized plateaus in the Hall resistance shown in Figs. 1(a) and 1(d). The minima of the second type (II) are shallower. They exist at integer fillings of only a *particular layer* and appear only in either the front- or back-gate capacitance. For these minima, the Hall resistance is not quantized and only weak features are observable in the longitudinal resistance. Examples of such minima for the front layer have been marked on the $C_{FG,norm}$ curves by upward triangles in panels (b) and (c) of Fig. 1. The corresponding integer filling factor values, ν_{FL}, have been included. For the minima in the C_{BG} curve and determination of filling factors we refer to Ref. [25] and the Supplemental Material [29]. Note also a fractional incompressible state at $\nu_{FL} = 2/3$.
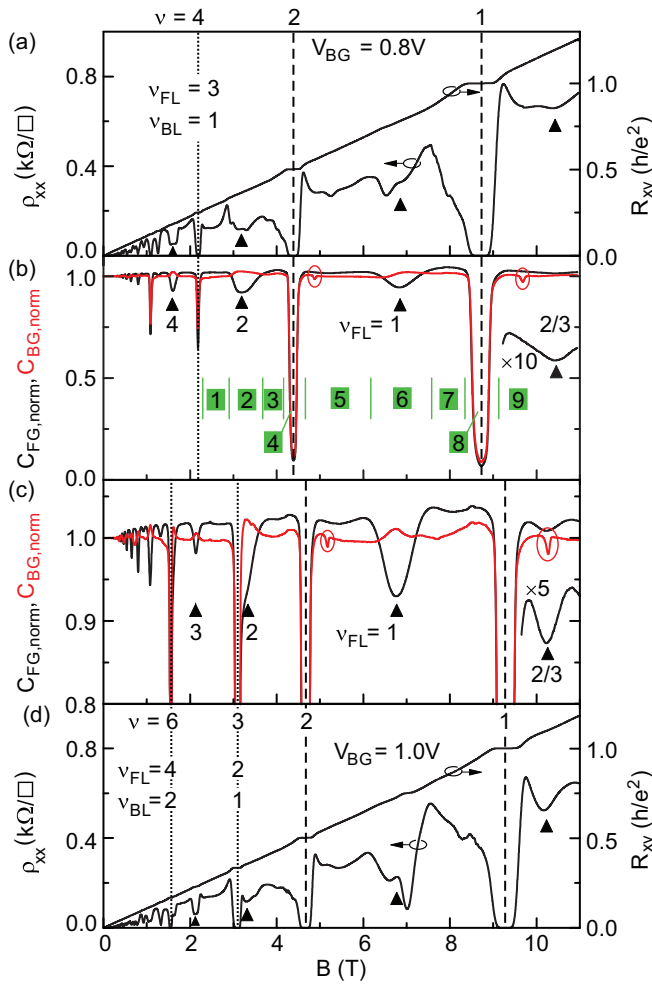
FIG. 1. Magnetoresistivity ρ_{xx} and Hall resistance R_{xy} for $V_{BG} = 0.8$ V (a) and 1.0 V (d). The normalized capacitances $C_{FG,norm}$ for these back gate voltages are shown as black curves in (b) and (c), respectively, together with $C_{BG,norm}$ (red curves). Data were recorded for $V_{FG} = -0.2$ V and $T = 0.5$ K. Note the different vertical scales in panels (b) and (c). Vertical dotted or dashed lines mark QH states at the indicated total fillings ν. Where applicable, also integer fillings of the front (ν_{FL}) and back layer (ν_{BL}) have been specified. Upward triangles highlight minima in $C_{FG,norm}$ where only the front layer becomes incompressible. The filling ν_{FL} has been included near each triangle. The same positions are also marked in the magnetotransport panels (a) and (d). B-field ranges with qualitatively different compressibility in the layers are demarcated by green lines and labeled with consecutive numbers in (b).

If the filling factor of each layer is close to integer, the minima in both magnetocapacitances can incidentally merge, giving rise to deeper and narrower minima. These are minima of the third type (III). They occur for total filling $\nu > 2$ and are also accompanied by integer QH effect behavior in the longitudinal and Hall resistance. Some of these are marked by dotted lines, together with the total integer filling and the integer filling of each layer. All previously discussed minima stem from the sample area underneath the front gate. However, there are also a few weak minima (type IV) in $C_{BG,norm}$ which originate from incompressible states at filling 1 and 2 in the device area
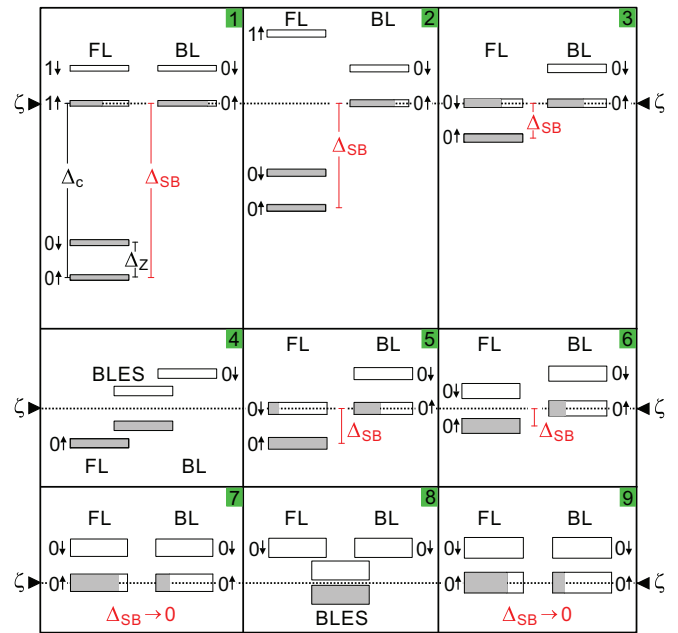

FIG. 2. Schematic of the Landau levels (rectangles with the level index and spin orientation) in the front layer (FL), back layer (BL), and the bilayer as a single entity (BLES) (in the vicinity of the electrochemical potential ς only). The panel numbers correspond to those of the B-field regions in Fig. 1(b). The area of the rectangles, representing Landau levels, is proportional to the level degeneracy (i.e., the magnetic field value), while the field dependence of the cyclotron (Δ_c) and Zeeman splitting (Δ_Z) is omitted. The shaded area reflects the occupation of a level. Δ_{SB} is the subband splitting.

covered only by the back gate. These type-IV minima have been encircled in Fig. 1 and will not be discussed further.

A comparison of the two data sets for the different V_{BG} (upper and lower pair of panels in Fig. 1) shows that the incompressible states at total filling $\nu = 1$ and 2 (type I minima) and integer ν_{FL} (type II minima) are stable when the total density and the distribution of the charge carriers among the two layers is varied. Their B-field position simply changes in accordance with the relevant density. In contrast, the type-III minima associated with QH states for $\nu > 2$ crucially depend on these parameters. Specifically, the states with $\nu = 4 = \nu_{FL} + \nu_{BL} = 3 + 1$, ($\nu = 3 = 2 + 1$ and $\nu = 6 = 4 + 2$) appear only in the upper (lower) pair of panels, respectively. This corroborates that the observed $\nu > 2$ QH states are just a combination of two separate integer states in the individual layers with only a minor role of many-body effects in their formation. This result for the $\nu = 4$ QH state in our sample is different from the conclusions in Ref. [24].

The successful identification of these different types of minima enables magnetic field ranges to be assigned where either the front layer or the bilayer system as a whole forms an incompressible ground state or not. For the data in Fig. 1(b), these ranges are separated by short green vertical lines and labeled by consecutive numbers. It is possible to draw a diagram with the spin-split Landau levels of each layer (subband), their full or partial occupation, as well as their position relative to the electrochemical potential ς. In Fig. 2, this exercise has been carried out for regions 1–9 in Fig. 1(b). In these

nine regions, the back layer is compressible, $\nu_{BL} < 1$, and the chemical potential is always pinned in the lowest partially occupied Landau level of this layer, except for regions 4 and 8 which should be excluded, since here a true bilayer incompressible state forms. The front layer is compressible in regions 1, 3, 5, 7, and 9, and either the first (regions 7, 9), second (regions 3, 5), or third (region 1) level is partially filled. Incompressible ground states develop in the front layer at integer filling factors $\nu_{FL} = 2$ (region 2) and 1 (region 6). The incompressible states at $\nu = 1$ and 2 (regions 8 and 4) of the whole BLES cannot be understood in the single-particle Landau-level picture of the two separate layers, it requires the introduction of common levels for the whole system.

From the diagrams in Fig. 2, two important observations can be made: (i) The subband splitting Δ_{SB}, apparent from the distance between the lowest level of each layer, drops with increasing magnetic field. This is obvious from the evolution of the level alignment in panels 1, 3, 5, 7, and 9. This is due to the redistribution of electrons among the layers and the impact this has on the shape of the wide potential well. This electron redistribution and the accompanying subband splitting variation were first established for large filling factors in theoretical calculations [31,32] and then by optical [33,34], magneto-transport [35], and magnetocapacitance [36,37] experiments. The significance of this effect is, however, still frequently ignored. In the asymmetric BLES here, the splitting can be suppressed drastically by the magnetic field, almost down to zero on the scale set by the level spacing (see panels 7 and 9 in Fig. 2). Quantitative estimates of this density redistribution are presented in the Supplemental Material [29]. Near total filling factor $\nu = 2$, the lowest Landau levels of each layer with opposite spin are aligned (panels 3 and 5 in Fig. 2). This is the key prerequisite for the formation of a canted antiferromagnetic phase. Also near $\nu = 1$, Landau levels of each layer align (panels 7 and 9 in Fig. 2). Within a single-particle picture, one may anticipate a continuous evolution between the compressible states shown in panels 3 and 5, as well as 7 and 9, due to a smooth variation of the level fillings. (ii) However, instead, an incompressible state emerges at $\nu = 2$ and 1 in between these states (panels 4 and 8). The relative occupation of the aligned levels does not seem to matter as apparent from measurements at different V_{BG} in Fig. 1. At these fillings, the bilayer system must be treated as a single entity with its own spectrum gapped at the electrochemical potential. The magnetic field induces a double quantum phase transition where the system mutates from compressible double layer to incompressible single-layer-like and back to compressible double layer. This is seen in sequence 3-4-5 as well as 7-8-9 in Fig. 2.

With the capacitance technique used here, it is possible to additionally verify that at $\nu = 1$ and 2, the bilayer system acts as one entity rather than two layers. To this end, it is instructive to consider the equations for the front- and back-gate capacitance for a single-layer system [37]:

$$C_{FG(BG)}^{-1} = \frac{d_{FG(BG)}}{\epsilon_0 \epsilon S} + \frac{1}{e^2 S}\left(1 + \frac{d_{FG(BG)}}{d_{BG(FG)}}\right)D^{-1}. \quad (2)$$

Here d_{FG} and d_{BG} are the distances between the 2DES and the front and back gate, respectively, $\epsilon_0 \epsilon$ is the dielectric constant of the material separating the 2DES and the gate,
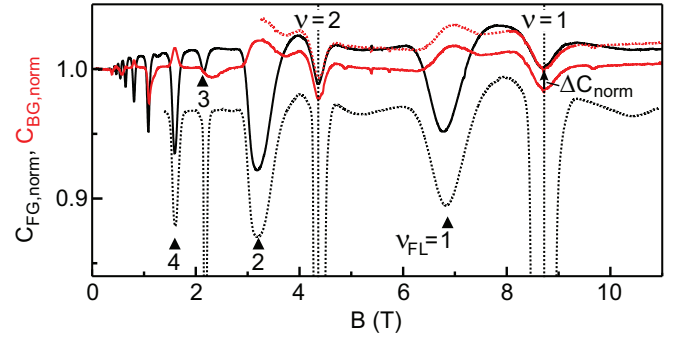

FIG. 3. Normalized magnetocapacitance $C_{FG,norm}$ (black) and $C_{BG,norm}$ (red) measured at $T = 1.5$ K and $V_{FG} = -0.2$ V in the presence of the back layer ($V_{BG} = 0.8$ V). $C_{FG,norm}$, measured at $T = 0.5$ K, is also shown (bottom black dotted line). For the sake of clarity, the curve is shifted downward. The red dotted line is a fragment of the $C_{BG,norm}$ trace shifted upwards by an amount equal to $\Delta C_{norm} = 0.015$ until the $\nu = 1$ and 2 minima coincide with those in $C_{FG,norm}$.

and S is the gated area. This equation differs from that of a field effect transistor with a single gate [30], because in the last term the ratio $d_{FG(BG)}/d_{BG(FG)}$ appears. For the normalized capacitances one then obtains identical equations:

$$C_{FG,norm}(B) = C_{BG,norm}(B)$$
$$= \frac{1 + (\epsilon_0 \epsilon/e^2)(d_{FG}^{-1} + d_{BG}^{-1})D^{-1}(B=0)}{1 + (\epsilon_0 \epsilon/e^2)(d_{FG}^{-1} + d_{BG}^{-1})D^{-1}(B)}. \quad (3)$$

This equality between normalized capacitances has been verified in an experiment at $V_{BG} = 0$ V, where only a front layer (ground subband) was occupied (the corresponding results are provided in the Supplemental Material [29]). Hence, in general, the key experimental signature that a double-sided gated 2D electron system acts as a single layer, even though it is composed of two layers, is that the normalized capacitances behave identically. In the data of Figs. 1(b) and 1(c), this holds true for the type-I capacitance minima at total filling $\nu = 1$ and 2 but not elsewhere. To corroborate this further, we present in Fig. 3 capacitance data measured at 1.5 K where the minima at $\nu = 1$ and 2 are not distorted by resistive effects [29,38] (see Supplemental Material) and Eqs. (2) and (3) are valid. The $\nu = 1$ and 2 minima in $C_{FG,norm}$ and $C_{BG,norm}$ now coincide in amplitude. This amplitude is also nearly the same for both fillings. A small vertical shift ΔC_{norm} is needed to truly superimpose the minima. This shift is identical for both minima. We attribute it to a change of the electron wave function when the electronic system converts from a double-layer to a single-layer-like configuration. These observations also confirm the similarity of the $\nu = 1$ and 2 incompressible states. The lower value of the minima in $C_{BG,norm}$ suggests an increase of the effective distance d_{BG} between the back gate and the electron system equal to $\Delta d_{BG} = \Delta C_{norm} d_{BG} \approx 13$ nm. This value is far less than the distance between the layers estimated as 34 nm (see the Supplemental Material [29]). Hence the single-layer-like states that form at total filling $\nu = 1$ and $\nu = 2$ are not centered at the location of either layer. Such behavior at $\nu = 2$ is not consistent with the easy-axis ferromagnetism scenario [24]. Instead, all our findings

for the $\nu = 1$ and $\nu = 2$ incompressible states including the single-layer behavior in both the electron energy spectrum and the capacitive response are qualitatively consistent with the formation of a many-body state where electrons reside simultaneously in both layers due to easy-plane pseudospin anisotropy as described by the theory in Refs. [21–23]. While with transport measurements in a dual-gated WQW sample, it is indeed possible to distinguish whether the energy spectrum of an incompressible ground state is single-layer or double-layer-like, it is not possible to establish single- or double-layer behavior in the compressible phases surrounding that incompressible ground state. This is an important issue successfully addressed here with these capacitance measurements.

IV. SUMMARY

In conclusion, we have studied an imbalanced bilayer electron system residing in an asymmetrical double-sided gated wide quantum well. With the help of magnetocapacitance measurements, it was possible to unequivocally identify magnetic field induced quantum phase transitions between double-layer states that can be interpreted in terms of the occupation of two Landau-level ladders and true single-layer-like incompressible ground states requiring a gapped spectrum for the system as a whole, independent of the initial distribution of the electrons between the layers. It was also possible to track the alignment of the partially filled Landau levels of the different layers at the electrochemical potential and the evolution of the subband splitting with magnetic field, which tends to zero in the quantum limit.

[1] I. B. Spielman, J. P. Eisenstein, L. N. Pfeiffer, and K. W. West, Phys. Rev. Lett. **84**, 5808 (2000).

[2] M. Kellogg, J. P. Eisenstein, L. N. Pfeiffer, and K. W. West, Phys. Rev. Lett. **93**, 036801 (2004).

[3] E. Tutuc, M. Shayegan, and D. A. Huse, Phys. Rev. Lett. **93**, 036802 (2004).

[4] R. D. Wiersma, J. G. S. Lok, S. Kraus, W. Dietsche, K. von Klitzing, D. Schuh, M. Bichler, H.-P. Tranitz, and W. Wegscheider, Phys. Rev. Lett. **93**, 266805 (2004).

[5] J. P. Eisenstein and A. H. MacDonald, Nature (London) **432**, 691 (2004).

[6] J. P. Eisenstein, Annu. Rev. Condens. Matter Phys. **5**, 159 (2014).

[7] L. Zheng, R. J. Radtke, and S. Das Sarma, Phys. Rev. Lett. **78**, 2453 (1997).

[8] S. Das Sarma, S. Sachdev, and L. Zheng, Phys. Rev. Lett. **79**, 917 (1997).

[9] A. H. MacDonald, R. Rajaraman, and T. Jungwirth, Phys. Rev. B **60**, 8817 (1999).

[10] Z. F. Ezawa, M. Eliashvili, and G. Tsitsishvili, Phys. Rev. B **71**, 125318 (2005).

[11] V. Pellegrini, A. Pinczuk, B. S. Dennis, A. S. Plaut, L. N. Pfeiffer, and K. W. West, Phys. Rev. Lett. **78**, 310 (1997).

[12] V. Pellegrini, A. Pinczuk, B. S. Dennis, A. S. Plaut, L. N. Pfeiffer, and K. W. West, Science **281**, 799 (1998).

[13] A. Sawada, Z. F. Ezawa, H. Ohno, Y. Horikoshi, Y. Ohno, S. Kishimoto, F. Matsukura, M. Yasumoto, and A. Urayama, Phys. Rev. Lett. **80**, 4534 (1998).

[14] A. Fukuda, A. Sawada, S. Kozumi, D. Terasawa, Y. Shimoda, Z. F. Ezawa, N. Kumada, and Y. Hirayama, Phys. Rev. B **73**, 165304 (2006).

[15] S. J. Geer, A. G. Davies, C. H. W. Barnes, K. R. Zolleis, M. Y. Simmons, and D. A. Ritchie, Phys. Rev. B **66**, 045318 (2002).

[16] V. S. Khrapai, E. V. Deviatov, A. A. Shashkin, V. T. Dolgopolov, F. Hastreiter, A. Wixforth, K. L. Campman, and A. C. Gossard, Phys. Rev. Lett. **84**, 725 (2000).

[17] N. Kumada, K. Muraki, and Y. Hirayama, Science **313**, 329 (2006).

[18] N. Kumada, K. Muraki, and Y. Hirayama, Phys. Rev. Lett. **99**, 076805 (2007).

[19] Y. W. Suen, J. Jo, M. B. Santos, L. W. Engel, S. W. Hwang, and M. Shayegan, Phys. Rev. B **44**, 5947 (1991).

[20] J. P. Eisenstein, L. N. Pfeiffer, and K. W. West, Appl. Phys. Lett. **57**, 2324 (1990).

[21] K. Yang, K. Moon, L. Zheng, A. H. MacDonald, S. M. Girvin, D. Yoshioka, and S-C. Zhang, Phys. Rev. Lett. **72**, 732 (1994).

[22] T. Jungwirth and A. H. MacDonald, Phys. Rev. B **63**, 035305 (2000).

[23] S. M. Girvin and A. H. MacDonald, in *Perspectives on Quantum Hall Effects*, edited by S. Das Sarma and A. Pinczuk (Wiley, New York, 1997).

[24] V. Piazza, V. Pellegrini, F. Beltram, W. Wegscheider, T. Jungwirth, and A. H. MacDonald, Nature (London) **402**, 638 (1999).

[25] S. I. Dorozhkin, A. A. Kapustin, I. B. Fedorov, V. Umansky, K. von Klitzing, and J. H. Smet, J. Appl. Phys. **123**, 084301 (2018).

[26] B. M. Hunt, J. I. A. Li, A. A. Zibrov, L. Wang, T. Taniguchi, K. Watanabe, J. Hone, C. R. Dean, M. Zaletel, R. C. Ashoori, and A. F. Young, Nat. Commun. **8**, 948 (2017).

[27] M. A. Mueed, D. Kamburov, S. Hasdemir, M. Shayegan, L. N. Pfeiffer, K. W. West, and K. W. Baldwin, Phys. Rev. Lett. **114**, 236406 (2015).

[28] M. A. Mueed, D. Kamburov, L. N. Pfeiffer, K. W. West, K. W. Baldwin, and M. Shayegan, Phys. Rev. Lett. **117**, 246801 (2016).

[29] See Supplemental Material at http://link.aps.org/supplemental/10.1103/PhysRevB.102.235307 for further information on the charge carrier population of each layer, the identification of the relevant contributions to the capacitances of this double-gated sample, and the experimental verification of Eq. (3).

[30] T. P. Smith, B. B. Goldberg, P. J. Stiles, and M. Heiblum, Phys. Rev. B **32**, 2696 (1985).

[31] J. Sanchez-Dehesa, F. Meseguer, F. Borondo, and J. C. Maan, Phys. Rev. B **36**, 5070 (1987).

[32] S. Trott, G. Paasch, G. Gobsch, and M. Trott, Phys. Rev. B **39**, 10232 (1989).

[33] D. G. Hayes, M. S. Skolnick, D. M. Whittaker, P. E. Simmonds, L. L. Taylor, S. J. Bass, and L. Eaves, Phys. Rev. B **44**, 3436 (1991).

[34] V. V. Solovyev, S. Schmult, W. Dietsche, and I. V. Kukushkin, Phys. Rev. B **80**, 241310(R) (2009).

[35] A. G. Davies, C. H. W. Barnes, K. R. Zolleis, J. T. Nicholls, M. Y. Simmons, and D. A. Ritchie, Phys. Rev. B **54**, R17331 (1996).

[36] S. I. Dorozhkin, JETP Lett. **103**, 513 (2016) [Pis'ma Zh. Eksp. Teor. Fiz. **103**, 578 (2016)].

[37] A. A. Kapustin, S. I. Dorozhkin, I. B. Fedorov, V. Umansky, and J. H. Smet, JETP Lett. **110**, 424 (2019) [Pis'ma Zh. Eksp. Teor. Fiz. **110**, 407 (2019)].

[38] S. I. Dorozhkin, A. A. Shashkin, N. B. Zhitenev, and V. T. Dolgopolov, JETP Lett. **44**, 241 (1986) [Pis'ma Zh. Eksp. Teor. Fiz. **44**, 189 (1986)].